

Accepted Manuscript

Structural optimization elaborates novel potent Akt inhibitors with promising anticancer activity

Yang Liu, Yanzhen Yin, Zhen Zhang, Carrie J. Li, Hui Zhang, Daoguang Zhang, Changying Jiang, Krystle Nomie, Liang Zhang, Michael L. Wang, Guisen Zhao



PII: S0223-5234(17)30521-4

DOI: [10.1016/j.ejmech.2017.06.067](https://doi.org/10.1016/j.ejmech.2017.06.067)

Reference: EJMECH 9562

To appear in: *European Journal of Medicinal Chemistry*

Received Date: 20 February 2017

Revised Date: 18 April 2017

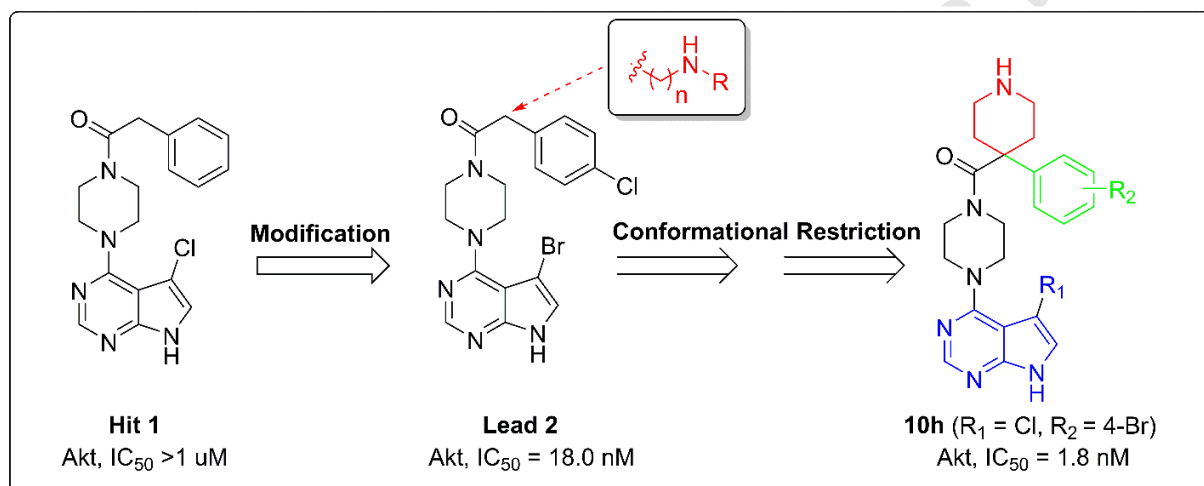
Accepted Date: 29 June 2017

Please cite this article as: Y. Liu, Y. Yin, Z. Zhang, C.J. Li, H. Zhang, D. Zhang, C. Jiang, K. Nomie, L. Zhang, M.L. Wang, G. Zhao, Structural optimization elaborates novel potent Akt inhibitors with promising anticancer activity, *European Journal of Medicinal Chemistry* (2017), doi: 10.1016/j.ejmech.2017.06.067.

This is a PDF file of an unedited manuscript that has been accepted for publication. As a service to our customers we are providing this early version of the manuscript. The manuscript will undergo copyediting, typesetting, and review of the resulting proof before it is published in its final form. Please note that during the production process errors may be discovered which could affect the content, and all legal disclaimers that apply to the journal pertain.

Graphic Abstract

Structural optimization produced a novel series of pyrrolopyrimidine based phenylpiperidine carboxamides as potent Akt inhibitors. Notably, **10h** exhibited robust antiproliferative effects in both mantle cell lymphoma cell lines and primary patient tumor cells.



Structural optimization elaborates novel potent Akt inhibitors with promising anticancer activity

Yang Liu¹, Yanzhen Yin¹, Zhen Zhang¹, Carrie J Li², Hui Zhang², Daoguang Zhang¹, Changying Jiang², Krystle Nomie², Liang Zhang², Michael L. Wang^{2,*} and Guisen Zhao^{1,*}

¹*Department of Medicinal Chemistry, Key Laboratory of Chemical Biology (Ministry of Education), School of Pharmaceutical Sciences, Shandong University, Jinan, Shandong 250012, PR China;*

²*The University of Texas MD Anderson Cancer Center, Houston, TX 77030, USA.*

Corresponding authors

Guisen Zhao*

Department of Medicinal Chemistry, School of Pharmaceutical Sciences, Shandong University, Jinan, Shandong 250012, PR China;

Tel/ Fax: +86 531 88382009;

E-mail: guisenzhao@sdu.edu.cn.

Michael L. Wang*

The University of Texas MD Anderson Cancer Center, Houston, TX 77030, USA.

Tel: +1 7137922860

Fax: +1 7137945656

E-mail: miwang@mdanderson.org

Abstract

Targeting of Akt has been validated as a well rationalized approach to cancer treatment, and represents a promising therapeutic strategy for aggressive hematologic malignancies. We describe herein an exploration of novel Akt inhibitors for cancer therapy through structural optimization of previously described 4-(piperazin-1-yl)-7*H*-pyrrolo[2,3-*d*]pyrimidine derivatives. Our studies yielded a novel series of pyrrolopyrimidine based phenylpiperidine carboxamides capable of potent inhibition of Akt1. Notably, **10h** exhibited robust antiproliferative effects in both mantle cell lymphoma cell lines and primary patient tumor cells. Low micromolar doses of **10h** induced cell apoptosis and cell cycle arrest in G₂/M phase, and significantly downregulated the phosphorylation of Akt downstream effectors GSK3 β and S6 in Jeko-1 cells.

Keywords: Akt, Anticancer, Docking, Mantle cell lymphoma, Piperidyl, Pyrrolopyrimidines

1. Introduction

Akt, also called protein kinase B or PKB, is a serine/threonine kinase that acts as a central junction in the phosphoinositide 3-kinase (PI3K) – Akt signaling pathway [1]. This cascade plays a critical role in regulating cell survival and proliferation, oncogenesis and mechanisms of drug resistance [2, 3]. There are three closely related Akt isoforms, Akt1 (PKB α), Akt2 (PKB β) and Akt3 (PKB γ), all of which share significant sequence identity in the ATP-binding site [4]. Akt promotes cell proliferation through the phosphorylation of various substrates such as glycogen synthase kinase 3 (GSK-3), TSC1/2, NF- κ B, Bcl-2 family proteins and mammalian target of rapamycin complex 1 (mTORC1) [5, 6]. Aberrant Akt activation has been confirmed in various cancers, including both hematological neoplasms and solid tumors, often in correlation with resistance to chemotherapy [7, 8]. Therefore, targeting Akt is a well rationalized approach to cancer treatment [9].

Mantle cell lymphoma (MCL) is a subtype of Non-Hodgkin's Lymphoma (NHL) with poor prognosis [10]. Although MCL typically responds to conventional chemotherapy, most patients eventually experience disease progression [11]. Aberrant Akt activation has been implicated in MCL pathogenesis and survival [12, 13]. While no PI3KCA mutations have been reported as contributors to constitutive Akt activation, loss of tumor suppressor PTEN may be an underlying drive of constitutive Akt signaling in MCL [14]. Such findings support the possibility of Akt inhibition as a novel strategy for the treatment of MCL.

Multiple strategies have been adopted for the discovery of small molecules that target Akt,

including ATP- or substrate-competitive inhibitors and allosteric inhibitors [15]. Of these, ATP-competitive inhibitors have yielded the most promising results. Common interactions between the ATP-competitive inhibitors and Akt include a heteroaromatic ring which forms bidentate hydrogen bonds to residues Glu228 and Ala230 in the hinge region, a basic amino group that can form hydrogen bonding interactions with the acid hole formed by Glu234 and Glu278, and an aromatic group positioned in a hydrophobic pocket under the P-loop [16, 17].

Our laboratory has reported the development of a weak hit **1** from self-library screening into lead **2**, an ATP-competitive inhibitor with desirable antiproliferative effects in prostate cancer cell lines [18]. For further modification of **2**, we decided to introduce an amino functionality at the benzylic position, which was inspired by the common structural platform of ATP-competitive inhibitors. In this regard, using a well-established conformational restriction drug design strategy, a piperidyl moiety with more conformational rigidity was deliberately chosen and incorporated, elaborating a novel series of (4-(7*H*-pyrrolo[2,3-*d*]pyrimidin-4-yl)piperazin-1-yl)(4-phenylpiperidin-4-yl)methanones with enhanced inhibitory potency in both enzyme activity and cancer cell growth (**Fig. 1**).

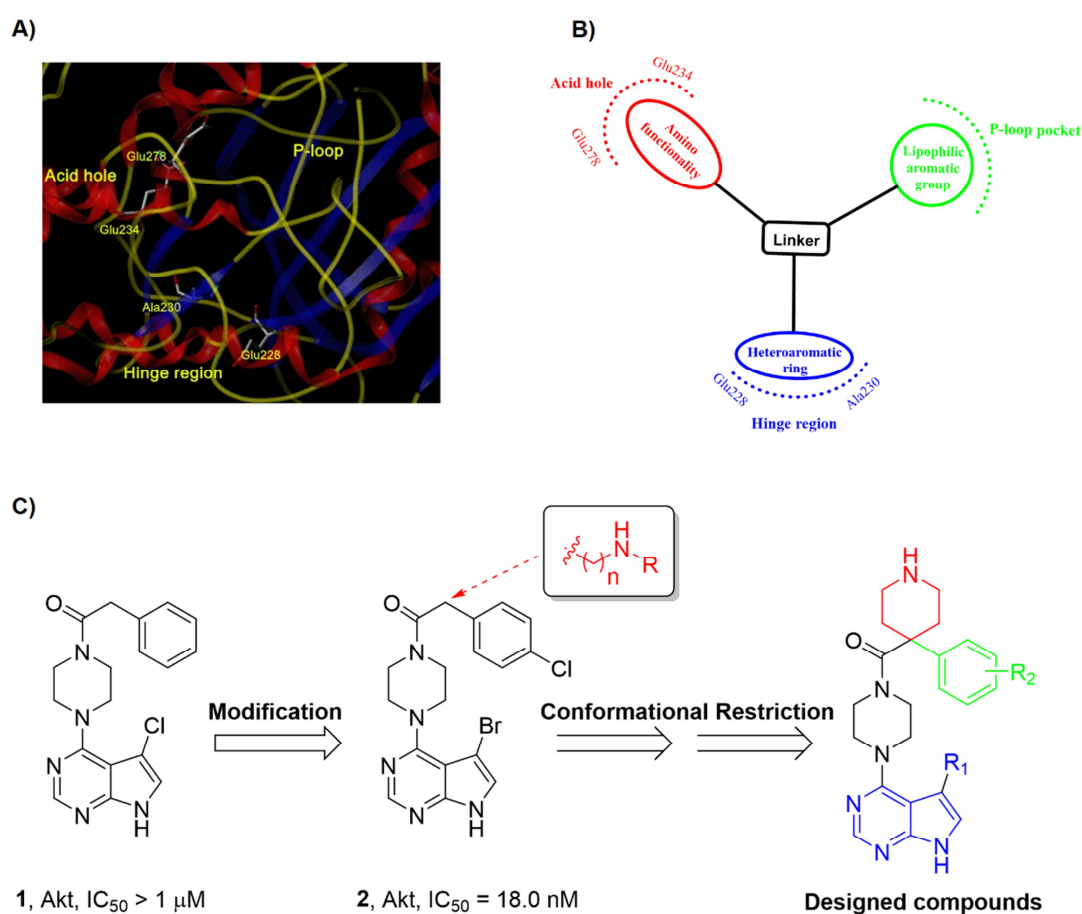
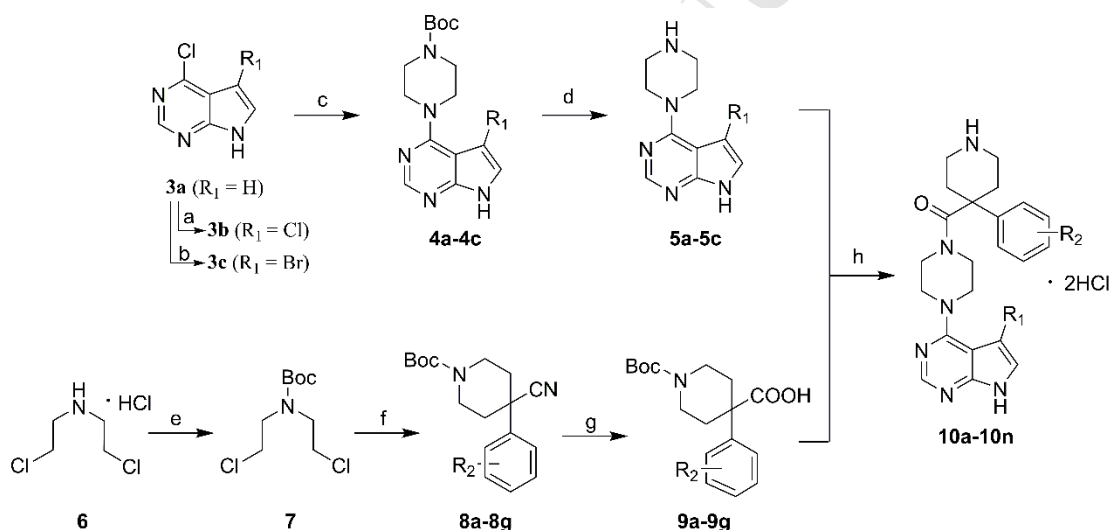


Fig. 1. Design of the targeted compounds. A) Binding site of the ATP-competitive inhibitors; B) common features of ATP-competitive inhibitors; C) Design of the targeted compounds from the initial hit **1**

2. Results and discussion

2.1. Chemistry

The general synthetic route for the pyrrolopyrimidine derivatives is outlined in **Scheme 1**. Chlorination or bromination at the 5-position of the readily available **3a** afforded compound **3b** or **3c**, subsequent introduction of the Boc-protected piperazine linker via S_NAr delivered **4a-4c**, followed by removal of the Boc group affording **5a-5c** as dihydrochloride salts. Commercially available **6** reacted with di-tert-butyl dicarbonate to produce the Boc-protected **7**, which was further used in the dialkylation of the substituted benzeneacetonitrile to afford intermediate **8a-8g**, basic hydrolysis of the nitrile **8a-8g** gave the carboxylic acid **9a-9g**. Amide coupling between **5a-5c** and **9a-9g** and deprotection of the Boc group achieved the target compounds **10a-10n**.



Scheme 1. Synthetic route for the designed derivatives. Reagents and conditions: (a) NCS, DMF, r.t.; (b) NBS, DMF, r.t.; (c) 1-Boc-piperazine, DIEA, DMF, 110°C; (d) HCl-dioxane, CH₃OH, r.t.; (e) (Boc)₂O, CH₂Cl₂, 10% NaOH (aq), r.t. (f) substituted benzeneacetonitrile, NaH, DMF, 60°C; (g) CH₃CH₂OH, NaOH(aq, 10M), 78°C; (h) (i) EDCl, HOBT, DIEA, DMF, r.t.; (ii) HCl-dioxane, CH₃OH, r.t..

2.2. Akt inhibition and cell antiproliferative activity

The fourteen newly synthesized pyrrolopyrimidine analogs were evaluated for their activity against Akt1 via a Homogeneous Time-Resolved Fluorescence (HTRF) kinase activity assay. Their effects on proliferation were further assessed in MCL cell lines. The first Akt inhibitor to enter clinical trials, GSK690693, served as a positive control. GSK690693 was previously shown to induce growth inhibition and apoptosis in acute lymphoblastic leukemia [19].

Table 1. The inhibitory effects of pyrrolopyrimidine derivatives on Akt1 activity

Code	R ₁	R ₂	Akt1, IC ₅₀ (nM) ^a	Code	R ₁	R ₂	Akt1, IC ₅₀ (nM) ^a
10a	H	4-tBu	> 40	10i	Cl	3,4-di-Cl	2.9 ± 0.9
10b	H	4-OCH ₃	35.6 ± 3.2	10j	Br	H	20.3 ± 1.6
10c	H	4-Cl	26.5 ± 0.7	10k	Br	3-Br	7.6 ± 2.0
10d	H	4-Br	27.1 ± 1.6	10l	Br	4-OCH ₃	14.1 ± 3.3
10e	H	3,4-di-Cl	> 40	10m	Br	4-Cl	1.5 ± 1.3
10f	Cl	3-Br	5.6 ± 2.5	10n	Br	3,4-di-Cl	4.3 ± 0.4
10g	Cl	4-Cl	1.9 ± 1.6			GSK690693	1.7 ± 1.1
10h	Cl	4-Br	1.8 ± 1.2			2	18.0 ^b

^aValues are means of three independent experiments;

^bValue for lead 2 was previously reported [18].

As **Table 1** shows, introduction of the piperidyl moiety at the benzylic position represented a substantial improvement in Akt1 inhibition over the initial lead (**2** vs **10m**). C5-substitution for chloro and bromo substituents produced an equivalent profile, with more than a 10-fold increase in enzyme inhibitory activity (**10c** vs **10g** and **10m**). Examination of substituents on the aromatic ring indicated that the chlorine or bromine substituent (**10k**, **10m** and **10n**) increased potency relative to the unsubstituted phenyl group of **10j**. The small decrease in enzyme potency for **10f** vs **10h** indicated that the *meta*-position was potentially less promising for manipulation; however, in the *para*-position, chloro and bromo analogues (**10g**, **10h** and **10m**) displayed similar levels of efficacy against Akt1 and showed the greatest enzyme potency comparable to that of **GSK690693**. A reduction in Akt1 potency was observed in the case of methoxy substitution (**10l**), whereas 3, 4-di-chloro substitution (**10i** and **10n**) was somewhat less active than the *p*-substitution (**10g** and **10m**).

The promising candidates **10h** and **10m** were further explored in a panel of MCL cell lines. As shown in **Table 2**, in comparison with the previous lead **2**, both compounds **10h** and **10m** demonstrated improved antiproliferative activities in MCL cell lines compared with **GSK690693**. **10h** was the most potent inhibitor in MCL cells with an IC₅₀ value lower than 1 μM.

Table 2. Cell proliferation assay assessing the effects of **10h** and **10m** on MCL cell lines

Code	Cell proliferation assay, IC ₅₀ ± SD/μM ^a					
	JVM-2	Maver-1	SP-49	Z-138	Mino	Jeko-1
2	9.9±0.7	18.5±2.2	7.8±1.0	6.8±0.5	18.1±2.6	8.7±1.3
10h	0.7±0.4	0.3±0.1	1.5±0.3	0.2±0.1	0.7±0.1	0.3±0.1
10m	2.3±1.3	1.8±0.4	4.7±0.1	1.7±0.3	3.5±0.3	1.2±0.1
GSK690693	1.6±0.7	5.1±0.5	4.8±0.1	3.1±0.2	20.8±3.5	3.0±1.5

^aValues are means of three independent experiments

2.3. Cell apoptosis and cell cycle assay

Activated Akt influences many factors that mediate apoptosis and the cell cycle [20]. Accordingly, apoptosis and cell cycle assays were performed after **10h** treatment in MCL Jeko-1 cells, which are characterized by constitutive phosphorylation of Akt and PTEN loss [21]. Annexin V/PI staining showed that **10h** induced cell apoptosis in Jeko-1 cells in a dose- and time-dependent manner (**Fig. 2**). Caspase-3 and PARP cleavage were measured to further confirm the initiation of apoptosis, and the results revealed dose-dependent activation of cleaved PARP and caspase-3 in Jeko-1 cells, indicating that **10h** induced cell apoptosis through the caspase 3-mediated PARP apoptotic pathway. The cell cycle assay demonstrated that treatment with **10h** dose dependently induced the cell cycle arrest in the G₂/M phase after 24 hours of treatment, effectively preventing cell cycle progression and promoting cell death.

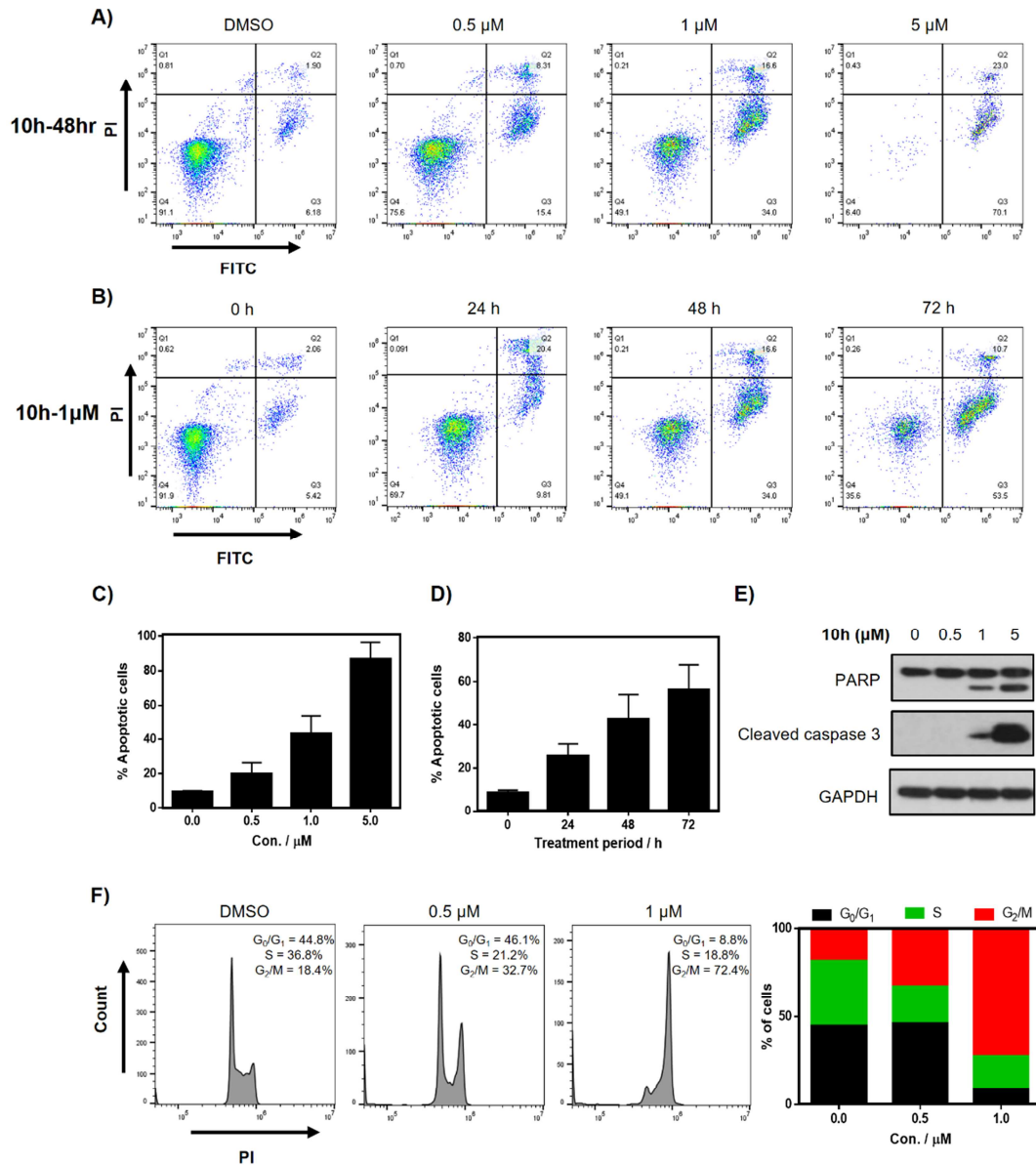


Fig. 2. Cell apoptosis and cell cycle assay for **10h** in Jeko-1 cells. A/C) Apoptosis assay of **10h** at indicated concentrations in Jeko-1 cells for 48 hours; B/D) Apoptosis assay of **10h** at 1 μ M in Jeko-1 cells for the indicated treatment periods; E) Dose-dependent activation of cleaved caspase-3 and PARP after 24 hours treatment with **10h**; F) Cell cycle analysis of **10h** at indicated concentrations in Jeko-1 cells for 24 hours.

2.4. Inhibitory effects on Akt signaling

To further examine the inhibitory effects of **10h** on Akt signaling, immunoblotting was performed to detect the phosphorylation of Akt and its downstream effectors GSK3 β and S6 in Jeko-1 cells (**Fig. 3A&B**). After 24 hours of **10h** treatment, phosphorylated GSK3 β and S6 levels were downregulated in a dose-dependent manner, while Ser473 and Thr308 phosphorylation of Akt was observed. These results are consistent with reported mechanisms of other Akt inhibitors, which point to a positive feedback mechanism as a mechanism for increased Akt phosphorylation [22-24].

2.5. Cell viability assay in primary MCL cells

The antiproliferative efficacy of the lead **2**, **10h**, **10m** and **GSK690693** were investigated in primary MCL patient cells. As shown in **Fig. 3C**, consistent with MCL cell lines, **10h** and **10m** dramatically decreased the cell viability of these cells in comparison to **GSK690693**.

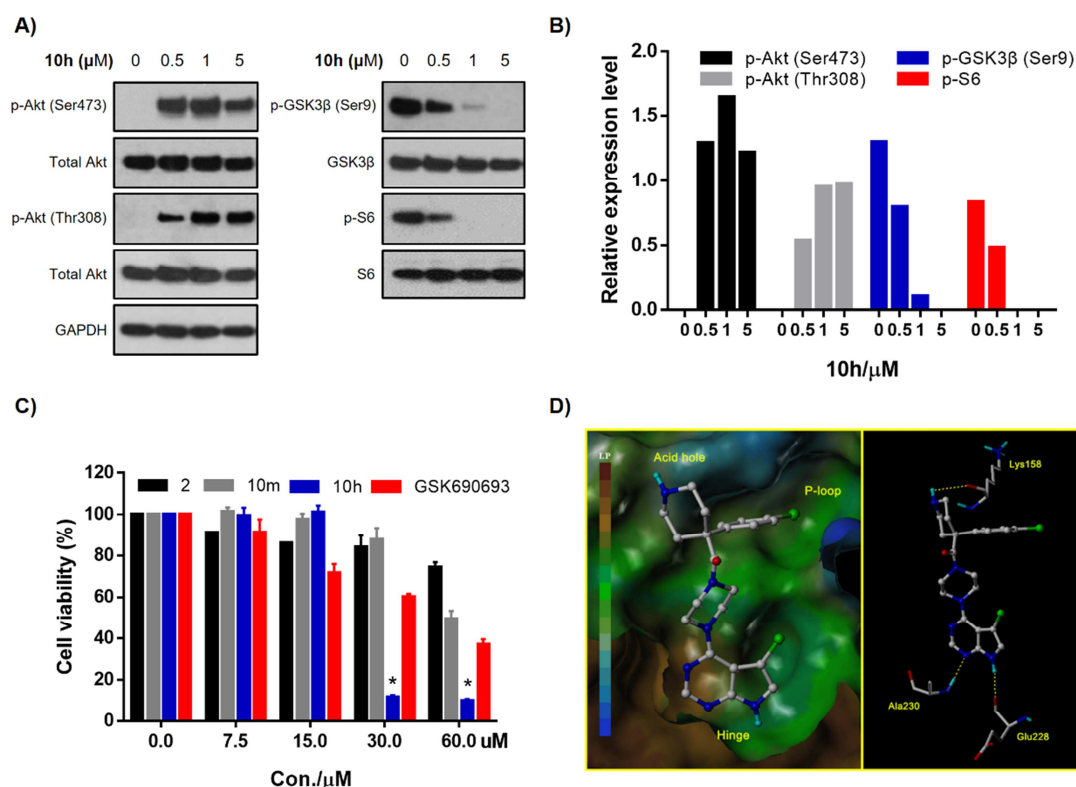


Fig. 3. Western blot analysis, cell viability assay in patient cells and molecular modeling. A) Effects of **10h** on Akt signaling in Jeko-1 cells after 24 hours treatment; B) Relative protein expression was determined using Image J. Values were normalized to loading control; C) Cell viability assay of **10h** in primary MCL cells. Values were normalized to control; Unpaired student's t-test between **10h** and **GSK690693**-treated cells is statistically significant (* $P < 0.01$); D) Proposed binding mode of **10h** at the ATP binding site of Akt1 (PDB: 4EKL).

2.6. Molecular modeling

The binding mode of **10h** was explored by molecular modeling using Sybyl 2.0 (**Fig. 3D**). As expected, the pyrrolopyrimidine core formed a pair of hydrogen bonds with the hinge region through Ala230 and Glu228, the 4-chlorophenyl group entered into a hydrophobic pocket under the P-loop. Instead of forming hydrogen bonds between Glu234 and Glu278 respectively within the acid hole, a different hydrogen bond was formed between the introduced piperidyl moiety and Lys158 to contribute to the binding potency to Akt enzyme.

3. Conclusion

In summary, we have described the optimization of previously reported pyrrolopyrimidine Akt

inhibitors to a series of advanced pyrrolopyrimidine based phenylpiperidine carboxamides.

Introduction of piperidyl moiety at the benzylic position resulted in a substantial boost in Akt1 inhibitory potency and antiproliferative effects in cancer cell growth, supporting further evaluation and development of the promising derivative **10h** in cancer therapy.

4. Experimental section

4.1. Chemistry

All solvents and reagents were purchased from commercial suppliers and used without further purification. All reactions were monitored by thin layer chromatography (TLC), and silica gel GF254 plates were used and visualized with UV light. Column chromatography was performed with silica gel using the solvents indicated. NMR spectra were recorded on a Bruker avance DRX600 or 400 Spectrometer using TMS as an internal standard in DMSO- d_6 . Chemical shifts are reported in parts per million (ppm). Coupling constants (J) are given in Hz. The mass spectra (MS) were measured with an API 4000. All of the melting points were determined in a Büchi capillary melting point apparatus and are uncorrected. Human Akt1 was obtained from Carna Biosciences, Inc. (Canada). The HTRF assay kit was purchased from Cisbio assays, Inc. (France).

4.2. General synthesis of compounds

4.2.1. General synthesis of compounds **3b** and **3c**

To a solution of readily available **3a** (20 mmol) in *N,N*-dimethylformamide (DMF) (15 mL) was added NCS/NBS (21 mmol) and the reaction mixture was stirred at room temperature for 72 h. Then ice water (150 mL) was poured into the mixture, the precipitate was filtered, washed with water (3×100 mL), and dried to give **3b** and **3c**.

4.2.1.1. 4, 5-Dichloro-7H-pyrrolo[2,3-d]pyrimidine (**3b**)

Grey powder, yield 95%, mp: 287~290°C, ^1H NMR (400 MHz, DMSO) δ (ppm): 12.87 (s, 1H), 8.63 (s, 1H), 7.91 (s, 1H). MS (ESI) m/z : 188 $[\text{M}+\text{H}]^+$.

4.2.1.2. 5-Bromo-4-chloro-7H-pyrrolo[2,3-d]pyrimidine (**3c**)

Pale powder, yield 95%, mp: 290~292°C, ^1H NMR (400 MHz, DMSO) δ (ppm): 13.00 (s, 1H), 8.64 (s, 1H), 7.97 (s, 1H). MS (ESI) m/z : 232 $[\text{M}+\text{H}]^+$.

4.2.2. General synthesis of compounds **4a-4c**

To a solution of **3a-3c** (3.2 mmol) and *N,N*-diisopropylethylamine (DIEA) (4.8 mmol) in DMF (3 mL) was added *N*-Boc-piperazine (3.6 mmol), the resulting mixture was heated at 110°C for 16 h. The

reaction mixture was poured into ice water (30 mL) and extracted with ethyl acetate (3×30 mL), the combined organic layers were washed with brine (2×30 mL), dried over sodium sulfate, filtered and concentrated under reduced pressure. The crude residue was purified by silica gel chromatography with petroleum ether/ethylacetate (1 : 3) to obtain **4a-4c**.

4.2.2.1. *Tert-butyl 4-(7H-pyrrolo[2,3-d]pyrimidin-4-yl)piperazine-1-carboxylate (4a)*

Off-white solid, yield 59%, ¹H NMR (600 MHz, DMSO) δ (ppm): 11.73 (s, 1H), 8.15 (s, 1H), 7.20 (d, *J* = 0.6 Hz, 1H), 6.64 (d, *J* = 1.8 Hz, 1H), 3.86 (s, 4H), 3.48 (s, 4H), 1.43 (s, 9H). MS (ESI) *m/z*: 304 [M+H]⁺.

4.2.2.2. *Tert-butyl 4-(5-chloro-7H-pyrrolo[2,3-d]pyrimidin-4-yl)piperazine-1-carboxylate (4b)*

Off-white solid, yield: 51%, ¹H NMR (400 MHz, DMSO) δ (ppm): 12.23 (s, 1H), 8.29 (s, 1H), 7.52 (d, *J* = 2.8 Hz, 1H), 3.52 (s, 8H), 1.42 (s, 9H). MS (ESI) *m/z*: 338 [M+H]⁺.

4.2.2.3. *Tert-butyl 4-(5-bromo-7H-pyrrolo[2,3-d]pyrimidin-4-yl)piperazine-1-carboxylate (4c)*

Pale yellow solid, yield 48%, ¹H NMR (400 MHz, DMSO) δ (ppm): 12.21 (s, 1H), 8.37 (s, 1H), 7.52 (d, *J* = 2.6 Hz, 1H), 3.52 (s, 8H), 1.42 (s, 9H). MS (ESI) *m/z*: 383 [M+H]⁺.

4.2.3. *General synthesis of compounds 5a-5c*

To a solution of **4a-4c** (1 mmol) suspended in methanol (1 ml) was added 4M HCl in dioxane (5 ml) and the reaction mixture was stirred for 24 h at room temperature. The precipitate was filtrated, washed with diethyl ether (2×5 ml), and dried to obtain **5a-5c**, which were used for the next step without further purification.

4.2.4. *Tert-butyl bis(2-chloroethyl)carbamate (7)*

To a solution of **6** (28.0 mmol) in dichloromethane (150 mL), 10% sodium hydroxide solution (33.6 mmol) was added. This was followed by addition of di-*tert*-butyl dicarbonate (33.6 mmol) over a period of 10 min at 0°C. After completion of the reaction, the organic layer was separated, washed with brine, dried over sodium sulfate and evaporated under reduced pressure. The crude product was purified by silica gel chromatography with petroleum ether/ethylacetate (8 : 1) to yield **7** as a pale yellow oil. Yield: 95%, ¹H NMR (600 MHz, DMSO) δ (ppm): 3.71-3.67 (m, 4H), 3.52 (t, *J* = 1.8 Hz, 4H), 1.40 (s, 9H). MS (ESI) *m/z*: 242 [M+H]⁺.

4.2.5. *General synthesis of compounds 8a-8g*

To a solution of **7** (1.66 mmol) and substituted benzeneacetonitrile (1.66 mmol) in anhydrous DMF (5 mL) was added NaH (60% dispersion in mineral oil, 8.4 mmol) portion wise at 0°C over 1 h.

The reaction mixture was heated at 60 °C for 16 h. The reaction mixture was poured into ice-water (50 mL) and extracted with ethyl acetate (3×50 mL). The combined organic layers were washed with brine (2×50 mL), dried over sodium sulfate, filtered, and concentrated. The crude product was purified by silica gel chromatography eluting with ether/ethyl ether (15:1) to give **8a-8g**.

4.2.5.1. *Tert-butyl 4-cyano-4-phenylpiperidine-1-carboxylate (8a)*

White solid, yield 30%, ¹H NMR (400 MHz, DMSO) δ (ppm): 7.55 (m, 2H), 7.44 (t, *J* = 7.8 Hz, 2H), 7.38 (d, *J* = 7.2 Hz, 1H), 4.13 (d, *J* = 13.2 Hz, 2H), 3.02 (br, 2H), 2.12 (d, *J* = 11.8 Hz, 2H), 1.92 (td, *J*₁ = 12.9 Hz, *J*₂ = 4.3 Hz, 2H), 1.42 (s, 9H). MS (ESI) *m/z*: 287 [M+H]⁺.

4.2.5.2. *1-Tert-butyl 4-(3-bromophenyl)-4-cyanopiperidine-1-carboxylate (8b)*

White solid, yield 63%, ¹H NMR (400 MHz, DMSO) δ (ppm): 7.74 (t, *J* = 1.76 Hz, 1H), 7.58 (td, *J*₁ = 7.76 Hz, *J*₂ = 1.5 Hz, 2H), 7.41 (t, *J* = 7.9 Hz, 1H), 4.13 (d, *J* = 13.0 Hz, 2H), 3.00 (br, 2H), 2.14 (d, *J* = 12.1 Hz, 2H), 1.90 (td, *J*₁ = 13.0 Hz, *J*₂ = 4.4 Hz, 2H), 1.42 (s, 9H). MS (ESI) *m/z*: 365 [M+H]⁺.

4.2.5.3. *Tert-butyl 4-(4-(tert-butyl)phenyl)-4-cyanopiperidine-1-carboxylate (8c)*

Pale yellow solid, yield 59%, ¹H NMR (400 MHz, DMSO) δ (ppm): 7.45 (s, 4H), 4.12 (d, *J* = 6.5 Hz, 2H), 3.01 (br, 2H), 2.10 (d, *J* = 6.2 Hz, 2H), 1.89 (td, *J*₁ = 13.1 Hz, *J*₂ = 4.2 Hz, 2H), 1.42 (s, 9H), 1.28 (s, 9H). MS (ESI) *m/z*: 343 [M+H]⁺.

4.2.5.4. *Tert-butyl 4-cyano-4-(4-methoxyphenyl)piperidine-1-carboxylate (8d)*

Pale yellow solid, yield 61%, ¹H NMR (400 MHz, DMSO) δ (ppm): 7.44 (d, *J* = 8.8 Hz, 2H), 6.98 (d, *J* = 8.76 Hz, 2H), 4.11 (d, *J* = 12.9 Hz, 2H), 3.76 (s, 3H), 3.01 (br, 2H), 2.09 (d, *J* = 12.8 Hz, 2H), 1.86 (td, *J*₁ = 13.0 Hz, *J*₂ = 4.1 Hz, 2H), 1.42 (s, 9H). MS (ESI) *m/z*: 317 [M+H]⁺.

4.2.5.5. *Tert-butyl 4-(4-chlorophenyl)-4-cyanopiperidine-1-carboxylate (8e)*

White solid, yield 51%, ¹H NMR (600 MHz, DMSO) δ (ppm): 7.58 (d, *J* = 8.4 Hz, 2H), 7.51 (d, *J* = 8.4 Hz, 2H), 4.12 (br, 2H), 3.00 (br, 2H), 2.12 (d, *J* = 13.2 Hz, 2H), 1.91 (td, *J*₁ = 12.9 Hz, *J*₂ = 4.2 Hz, 2H), 1.42 (s, 9H). MS (ESI) *m/z*: 321 [M+H]⁺.

4.2.5.6. *Tert-butyl 4-(4-bromophenyl)-4-cyanopiperidine-1-carboxylate (8f)*

White solid, yield 50%, ¹H NMR (400 MHz, DMSO) δ (ppm): 7.65 (d, *J* = 8.6 Hz, 2H), 7.52 (d, *J* = 8.6 Hz, 2H), 4.13 (d, *J* = 12.8 Hz, 2H), 3.01 (br, 2H), 2.12 (d, *J* = 12.8 Hz, 2H), 1.91 (td, *J*₁ = 13.1 Hz, *J*₂ = 4.2 Hz, 2H), 1.42 (s, 9H). MS (ESI) *m/z*: 365 [M+H]⁺.

4.2.5.7. *Tert-butyl 4-cyano-4-(3,4-dichlorophenyl)piperidine-1-carboxylate (8g)*

Pale yellow solid, yield 58%, ¹H NMR (400 MHz, DMSO) δ (ppm): 7.82 (d, *J* = 2.3 Hz, 1H), 7.72 (d, *J*

= 8.5 Hz, 1H), 7.57 (dd, $J_1 = 6.2$ Hz, $J_2 = 2.3$ Hz, 1H), 4.13 (d, $J = 13.1$ Hz, 2H), 3.02 (br, 2H), 2.15 (d, $J = 12.2$ Hz, 2H), 1.96 (m, 2H), 1.42 (s, 9H). MS (ESI) m/z: 355 [M+H]⁺.

4.2.6. General synthesis of compounds **9a-9g**

A solution of **8a-8g** (1.15 mmol) in ethanol (3 mL) and 3 mL 10 N aqueous sodium hydroxide was refluxed for 48 hours, cooled to room temperature, then poured into 1 N aqueous hydrochloric acid, and extracted by ethyl acetate. The organic extracts were washed with brine, dried over sodium sulfate, and concentrated under reduced pressure. The crude product was recrystallized using ethyl acetate to obtain **9a-9g**.

4.2.6.1. 1-(Tert-butoxycarbonyl)-4-phenylpiperidine-4-carboxylic acid (**9a**)

White solid, yield 73%, ¹H NMR (400 MHz, DMSO) δ (ppm): 12.70 (s, 1H), 7.40-7.33 (m, 4H), 7.28-7.24 (m, 1H), 3.80 (d, $J = 13.6$ Hz, 2H), 2.96 (br, 2H), 2.36 (d, $J = 13.2$ Hz, 2H), 1.73-1.67 (m, 2H), 1.39 (s, 9H). MS (ESI) m/z: 304 [M+H]⁺.

4.2.6.2. 4-(3-Bromophenyl)-1-(tert-butoxycarbonyl)piperidine-4-carboxylic acid (**9b**)

White solid, yield 78%, ¹H NMR (400 MHz, DMSO) δ (ppm): 12.87 (s, 1H), 7.52 (t, $J = 18.0$ Hz, 1H), 7.50-7.47 (m, 1H), 7.42-7.40 (m, 1H), 7.33 (t, $J = 7.8$ Hz, 1H), 3.79 (d, $J = 5.6$ Hz, 2H), 2.99 (br, 2H), 2.34 (d, $J = 13.6$ Hz, 2H), 1.75-1.67 (m, 2H), 1.39 (s, 9H). MS (ESI) m/z: 382 [M+H]⁺.

4.2.6.3. 1-(Tert-butoxycarbonyl)-4-(4-(tert-butyl)phenyl)piperidine-4-carboxylic acid (**9c**)

White solid, yield 67%, ¹H NMR (400 MHz, DMSO) δ (ppm): 12.62 (br, 1H), 7.36 (d, $J = 8.4$ Hz, 2H), 7.30 (d, $J = 8.4$ Hz, 2H), 3.80 (d, $J = 13.6$ Hz, 2H), 2.93 (br, 2H), 2.35 (d, $J = 13.6$ Hz, 2H), 1.71-1.64 (m, 2H), 1.38 (s, 9H), 1.25 (s, 9H). MS (ESI) m/z: 360 [M+H]⁺.

4.2.6.4. 1-(Tert-butoxycarbonyl)-4-(4-methoxyphenyl)piperidine-4-carboxylic acid (**9d**)

White solid, yield 57%, ¹H NMR (400 MHz, DMSO) δ (ppm): 12.58 (s, 1H), 7.30 (m, 2H), 6.91 (m, 2H), 3.78-3.72 (m, 5H), 2.95 (br, 2H), 2.33 (d, $J = 13.6$ Hz, 2H), 1.63-1.70 (m, 2H), 1.38 (s, 9H). MS (ESI) m/z: 334 [M+H]⁺.

4.2.6.5. 1-(Tert-butoxycarbonyl)-4-(4-chlorophenyl)piperidine-4-carboxylic acid (**9e**)

White solid, yield 80%, ¹H NMR (400 MHz, DMSO) δ (ppm): 12.80 (s, 1H), 7.41 (s, 4H), 3.77 (d, $J = 13.6$ Hz, 2H), 2.97 (br, 2H), 2.34 (d, $J = 13.6$ Hz, 2H), 1.74-1.67 (m, 2H), 1.39 (s, 9H). MS (ESI) m/z: 338 [M+H]⁺.

4.2.6.6. 4-(4-Bromophenyl)-1-(tert-butoxycarbonyl)piperidine-4-carboxylic acid (**9f**)

White solid, yield 68%, ¹H NMR (600 MHz, DMSO) δ (ppm): 12.81 (s, 1H), 7.55 (d, $J = 8.4$ Hz, 2H),

7.35 (d, $J = 8.4$ Hz, 2H), 3.77 (d, $J = 13.8$ Hz, 2H), 2.96 (br, 2H), 2.33 (d, $J = 13.8$ Hz, 2H), 1.72-1.67 (m, 2H), 1.39 (s, 9H). MS (ESI) m/z : 382 $[M+H]^+$.

4.2.6.7. 1-(Tert-butoxycarbonyl)-4-(3,4-dichlorophenyl)piperidine-4-carboxylic acid (**9g**)

White solid, yield 81%, ^1H NMR (400 MHz, DMSO) δ (ppm): 12.97 (s, 1H), 7.63 (d, $J = 8.2$ Hz, 1H), 7.59 (d, $J = 3.6$ Hz, 1H), 7.40 (dd, $J_1 = 8.2$ Hz, $J_2 = 2.0$ Hz, 1H), 3.76 (d, $J = 21.0$ Hz, 2H), 2.97 (br, 2H), 2.33 (d, $J = 20.4$ Hz, 2H), 1.77-1.70 (m, 2H), 1.39 (s, 9H). MS (ESI) m/z : 372 $[M+H]^+$.

4.2.7. General synthesis of compounds **10a-10n**

To a solution of **9a-9g** (0.30 mmol) and DIEA (3.0 mmol) in DMF (2 mL) was added 1-(3-dimethylaminopropyl)-3-ethylcarbodiimide hydrochloride (EDCI) (0.33 mmol) and 1-hydroxybenzotriazole (HOBt) (0.33 mmol). The reaction mixture was stirred at 0°C for 1 hour, followed by addition of **5a-5c** (0.30 mmol). After completion of addition, the final mixture was stirred at room temperature for another 12 hours, then poured into ice water (20 mL), washed with saturated aqueous sodium bicarbonate (20×3 mL) and brine (20×2 mL), dried over sodium sulfate and solvent was evaporated under reduced pressure. The residue was suspended in methanol (0.5 mL), after addition of the 4M HCl in dioxane (3 mL), the reaction mixture was stirred for 24 hours at room temperature. The precipitate was filtrated, the obtained solid was recrystallized from methanol to give the desired **10a-10n**.

4.2.7.1. (4-(7H-pyrrolo[2,3-d]pyrimidin-4-yl)piperazin-1-yl)(4-(4-(tert-butyl)phenyl)piperidin-4-yl)methanone (**10a**)

Palewhite solid, yield 69%, mp: 223~228°C, ^1H NMR (400 MHz, D_2O) δ (ppm): 8.14 (s, 1H), 7.47 (d, $J = 8.8$ Hz, 1H), 7.26-7.24 (m, 3H), 6.57 (d, $J = 3.6$ Hz, 1H), 3.98-3.81 (m, 4H), 3.41-3.23 (m, 8H), 2.52 (d, $J = 14.4$ Hz, 2H), 2.20 (t, $J = 11.6$ Hz, 2H), 1.19 (s, 9H). ^{13}C NMR (100 MHz, D_2O) δ (ppm): 174.07, 152.03, 151.74, 144.73, 142.35, 138.57, 126.59 (2C), 125.07 (2C), 124.11, 103.93, 102.07, 66.54 (2C), 62.49 (2C), 47.73 (2C), 41.54, 33.89, 31.52 (2C), 30.40 (3C). MS (ESI) m/z : 447 $[M+H]^+$.

4.2.7.2.

(4-(7H-pyrrolo[2,3-d]pyrimidin-4-yl)piperazin-1-yl)(4-(4-methoxyphenyl)piperidin-4-yl)methanone (**10b**)

Palewhite solid, yield 69%, mp: 215~220°C, ^1H NMR (400 MHz, D_2O) δ (ppm): 8.11 (s, 1H), 7.24 (d, $J = 3.6$ Hz, 1H), 7.19 (d, $J = 8.8$ Hz, 2H), 6.85 (d, $J = 8.8$ Hz, 2H), 6.55 (d, $J = 3.6$ Hz, 1H), 3.94-3.81 (m, 4H), 3.69 (s, 3H), 3.51-3.19 (m, 10H), 2.51 (d, $J = 10.8$ Hz, 2H), 2.16 (t, $J = 15.6$ Hz, 2H). ^{13}C

NMR (100 MHz, D₂O) δ (ppm): 174.24, 158.29, 151.91, 144.81, 142.37, 133.89, 126.63(2C), 124.18, 114.86 (2C), 103.89, 101.95, 66.61 (2C), 55.43 (3C), 47.54 (2C), 44.86 (2C), 41.63, 31.64 (2C). MS (ESI) m/z: 421 [M+H]⁺.

4.2.7.3. (4-(7H-pyrrolo[2,3-d]pyrimidin-4-yl)piperazin-1-yl)(4-(4-chlorophenyl)piperidin-4-yl)methanone (**10c**)

Palewhite solid, yield 67%, mp: 189~194°C, ¹H NMR (400 MHz, D₂O) δ (ppm): 8.12 (s, 1H), 7.52-7.22 (m, 5H), 6.55 (s, 1H), 3.95-3.83 (m, 4H), 3.45-3.24 (m, 8H), 2.50 (d, *J* = 10.8 Hz, 2H), 2.13 (s, 2H). ¹³C NMR (100 MHz, D₂O) δ (ppm): 173.55, 152.03, 144.51, 142.38, 140.19, 133.22, 129.56 (2C), 126.81 (2C), 124.30, 103.86, 101.92, 66.62 (2C), 62.60 (2C), 47.81 (2C), 41.57, 31.52 (2C). MS (ESI) m/z: 425 [M+H]⁺.

4.2.7.4. (4-(7H-pyrrolo[2,3-d]pyrimidin-4-yl)piperazin-1-yl)(4-(4-bromophenyl)piperidin-4-yl)methanone (**10d**)

White solid, yield 65%, mp: 253~257°C, ¹H NMR (400 MHz, D₂O) δ (ppm): 8.13 (s, 1H), 7.43 (d, *J* = 8.4 Hz, 2H), 7.27 (d, *J* = 4.0 Hz, 1H), 7.17 (d, *J* = 8.4 Hz, 2H), 6.56 (dd, *J* = 3.6 Hz, 1H), 3.96-3.83 (m, 4H), 3.47-3.38 (m, 6H), 3.27 (t, *J* = 11.6 Hz, 2H), 2.51 (d, *J* = 14.0 Hz, 2H), 2.16 (t, *J* = 12.0 Hz, 2H). ¹³C NMR (100 MHz, D₂O) δ (ppm): 173.51, 152.13, 144.60, 142.52, 140.70, 132.54 (2C), 127.14 (2C), 124.27, 121.37, 103.81, 101.95, 66.61 (2C), 62.54 (2C), 47.93 (2C), 41.53, 31.45 (2C). MS (ESI) m/z: 471 [M+H]⁺.

4.2.7.5. (4-(7H-pyrrolo[2,3-d]pyrimidin-4-yl)piperazin-1-yl)(4-(3,4-dichlorophenyl)piperidin-4-yl)methanone (**10e**)

Palewhite solid, yield 68%, mp: 195~199°C, ¹H NMR (400 MHz, D₂O) δ (ppm): 8.12 (s, 1H), 7.35 (d, *J* = 8.4 Hz, 1H), 7.32 (d, *J* = 2.4 Hz, 1H), 7.24 (d, *J* = 3.6 Hz, 1H), 7.16 (d, *J*₁ = 8.4 Hz, *J*₂ = 2.4 Hz, 1H), 6.49 (d, *J* = 3.6 Hz, 1H), 3.96-3.86 (m, 4H), 3.52-3.38 (m, 6H), 3.26 (t, *J* = 12.4 Hz, 2H), 2.51 (d, *J* = 14.4 Hz, 2H), 2.12 (t, *J* = 12.0 Hz, 2H). ¹³C NMR (100 MHz, D₂O) δ (ppm): 172.96, 152.07, 144.48, 142.47, 141.94, 132.95, 131.40 (2C), 127.27 (2C), 124.99, 124.39, 103.60, 101.76, 66.62 (2C), 47.98 (2C), 41.49 (2C), 34.60, 31.39 (2C). MS (ESI) m/z: 459 [M+H]⁺.

4.2.7.6.

(4-(3-bromophenyl)piperidin-4-yl)(4-(5-chloro-7H-pyrrolo[2,3-d]pyrimidin-4-yl)piperazin-1-yl)methanone (**10f**)

Paleyellow solid, yield 80%, mp: 257~261°C, ¹H NMR (400 MHz, D₂O) δ (ppm): 8.12 (s, 1H),

7.45-7.41 (m, 2H), 7.31 (s, 1H), 7.28-7.26 (m, 2H), 3.79 (br, 4H), 3.42-3.22 (m, 8H), 2.50 (t, $J = 14.0$ Hz, 2H), 2.18 (t, $J = 12.4$ Hz, 2H). ^{13}C NMR (100 MHz, D_2O) δ (ppm): 172.85, 153.46, 145.54, 144.12, 143.20, 139.15, 131.44, 130.96, 128.24, 123.51, 123.03, 104.89, 101.03, 57.43 (2C), 48.47 (2C), 48.02 (2C), 41.46, 31.56 (2C). MS (ESI) m/z : 505 $[\text{M}+\text{H}]^+$.

4.2.7.7. (4-(5-chloro-7H-pyrrolo[2,3-d]pyrimidin-4-yl)piperazin-1-yl)(4-(4-chlorophenyl)piperidin-4-yl) methanone (**10g**)

Palewhite solid, yield 66%, mp: 200~205°C, ^1H NMR (400 MHz, D_2O) δ (ppm): 8.11 (s, 1H), 7.33 (d, $J = 8.8$ Hz, 2H), 7.29 (s, 1H), 7.25 (d, $J = 8.4$ Hz, 2H), 3.85-3.69 (m, 4H), 3.41-3.22 (m, 8H), 2.50 (t, $J = 14.4$ Hz, 2H), 2.18 (t, $J = 12.0$ Hz, 2H). ^{13}C NMR (100 MHz, D_2O) δ (ppm): 173.26, 153.65, 145.83, 143.34, 140.48, 133.25, 129.63 (2C), 126.99 (2C), 123.65, 104.99, 101.26, 66.62 (2C), 62.61 (2C), 47.82 (2C), 41.55, 31.64 (2C). MS (ESI) m/z : 459 $[\text{M}+\text{H}]^+$.

4.2.7.8. (4-(4-bromophenyl)piperidin-4-yl)(4-(5-chloro-7H-pyrrolo[2,3-d]pyrimidin-4-yl)piperazin-1-yl) methanone (**10h**)

Paleyellow solid, yield 61%, mp: 203~208°C, ^1H NMR (400 MHz, D_2O) δ (ppm): 8.10 (s, 1H), 7.47 (d, $J = 8.6$ Hz, 2H), 7.28 (s, 1H), 7.19 (d, $J = 8.6$ Hz, 2H), 3.76 (s, 3H), 3.67 (s, 2H), 3.46-3.38 (m, 3H), 3.26 (t, $J = 11.9$ Hz, 3H), 3.11 (s, 2H), 2.49 (d, $J = 14.4$ Hz, 2H), 2.21-2.10 (m, 2H). ^{13}C NMR (100 MHz, D_2O) δ (ppm): 173.10, 153.92, 146.02, 143.77, 141.00, 132.57 (2C), 127.24 (2C), 123.45, 121.37, 104.74, 101.30, 66.58 (2C), 62.55, 47.84 (2C), 41.48 (2C), 31.55 (2C). MS (ESI) m/z : 505 $[\text{M}+\text{H}]^+$.

4.2.7.9.

(4-(5-chloro-7H-pyrrolo[2,3-d]pyrimidin-4-yl)piperazin-1-yl)(4-(3,4-dichlorophenyl)piperidin-4-yl) methanone (**10i**)

Palewhite solid, yield 65%, mp: 260~263°C, ^1H NMR (400 MHz, D_2O) δ (ppm): 8.11 (s, 1H), 7.44-7.40 (m, 2H), 7.28 (s, 1H), 7.20 (d, $J = 7.2$ Hz, 1H), 3.76 (br, 4H), 3.48-3.24 (m, 8H), 2.49 (d, $J = 10.8$ Hz, 2H), 2.13 (s, 2H). ^{13}C NMR (100 MHz, D_2O) δ (ppm): 172.67, 153.92, 145.98, 143.79, 142.28, 133.02, 131.55, 131.47, 127.41, 125.20, 123.56, 104.71, 101.19, 66.62 (2C), 62.06 (2C), 47.84 (2C), 41.47, 31.54 (2C). MS (ESI) m/z : 493 $[\text{M}+\text{H}]^+$.

4.2.7.10. (4-(5-bromo-7H-pyrrolo[2,3-d]pyrimidin-4-yl)piperazin-1-yl)(4-phenylpiperidin-4-yl) methanone (**10j**)

Palewhite solid, yield 63%, mp: 258~261°C, ^1H NMR (400 MHz, D_2O) δ (ppm): 8.10 (s, 1H), 7.36 (s, 1H), 7.23 (d, $J = 8.8$ Hz, 2H), 6.92-6.90 (m, 3H), 3.74-3.08 (m, 12H), 2.50 (d, $J = 14.8$ Hz, 2H), 2.16 (t,

$J = 11.6$ Hz, 2H). ^{13}C NMR (100 MHz, D_2O) δ (ppm): 173.88, 158.35, 154.08, 146.98, 143.36, 134.19, 126.76 (2C), 126.56, 114.98 (2C), 103.02, 88.94, 66.61 (2C), 55.50 (2C), 47.47 (2C), 41.60, 31.78 (2C). MS (ESI) m/z : 471 $[\text{M}+\text{H}]^+$.

4.2.7.11.

(4-(5-bromo-7H-pyrrolo[2,3-d]pyrimidin-4-yl)piperazin-1-yl)(4-(3-bromophenyl)piperidin-4-yl)methanone (10k)

Paleyellow solid, yield 63%, mp: 240~245°C, ^1H NMR (400 MHz, D_2O) δ (ppm): 8.11 (s, 1H), 7.45 (s, 1H), 7.42 (dd, $J_1 = 6.0$ Hz, $J_2 = 2.4$ Hz, 1H), 7.35 (s, 1H), 7.28-7.25 (m, 2H), 3.78-3.16 (m, 12H), 2.49 (d, $J = 14.4$ Hz, 2H), 2.19 (t, $J = 12.0$ Hz, 2H). ^{13}C NMR (100 MHz, D_2O) δ (ppm): 172.94, 154.32, 146.98, 144.17, 143.65, 131.50, 131.10, 128.34 (2C), 126.49 (2C), 124.21, 123.12, 103.05, 88.90, 66.62 (2C), 62.60 (2C), 48.06 (2C), 41.51, 31.62 (2C). MS (ESI) m/z : 549 $[\text{M}+\text{H}]^+$.

4.2.7.12.

(4-(5-bromo-7H-pyrrolo[2,3-d]pyrimidin-4-yl)piperazin-1-yl)(4-(4-methoxyphenyl)piperidin-4-yl)methanone (10l)

Palewhite solid, yield 62%, mp: 218~222°C, ^1H NMR (400 MHz, D_2O) δ (ppm): 8.06 (s, 1H), 7.29 (s, 1H), 7.20 (d, $J = 8.8$ Hz, 2H), 6.88 (d, $J = 8.8$ Hz, 2H), 3.72-3.01 (m, 15H), 2.48 (d, $J = 14.0$ Hz, 2H), 2.16 (t, $J = 12.0$ Hz, 2H). ^{13}C NMR (100 MHz, D_2O) δ (ppm): 173.79, 158.33, 154.29, 146.98, 143.76, 134.21, 126.73 (2C), 126.37, 114.95 (2C), 102.95, 88.74, 66.61 (2C), 62.60 (2C), 55.50 (3C), 47.46 (2C), 41.62, 31.80 (2C). MS (ESI) m/z : 501 $[\text{M}+\text{H}]^+$.

4.2.7.13.

(4-(5-bromo-7H-pyrrolo[2,3-d]pyrimidin-4-yl)piperazin-1-yl)(4-(4-chlorophenyl)piperidin-4-yl)methanone (10m)

Palewhite solid, yield 67%, mp: 252~257°C, ^1H NMR (400 MHz, D_2O) δ (ppm): 8.11 (s, 1H), 7.33 (s, 1H), 7.31 (d, $J = 8.4$ Hz, 2H), 7.25 (d, $J = 8.4$ Hz, 2H), 3.76-3.07 (m, 12H), 2.49 (d, $J = 13.6$ Hz, 2H), 2.17 (t, $J = 11.6$ Hz, 2H). ^{13}C NMR (100 MHz, D_2O) δ (ppm): 173.11, 154.25, 146.92, 143.64, 140.61, 133.19, 129.63 (2C), 127.03 (2C), 126.51, 102.99, 88.87, 66.62 (2C), 62.60 (2C), 47.80 (2C), 41.55, 31.66 (2C). MS (ESI) m/z : 505 $[\text{M}+\text{H}]^+$.

4.2.7.14.

(4-(5-bromo-7H-pyrrolo[2,3-d]pyrimidin-4-yl)piperazin-1-yl)(4-(3,4-dichlorophenyl)piperidin-4-yl)methanone (10n)

Paleyellow solid, yield 68%, mp: 248~251 °C, ¹H NMR (400 MHz, D₂O) δ (ppm): 8.10 (s, 1H), 7.44-7.42 (m, 2H), 7.31 (s, 1H), 7.20 (d, *J* = 7.2 Hz, 1H), 3.78-3.19 (m, 12H), 2.48 (d, *J* = 13.2 Hz, 2H), 2.16 (t, *J* = 11.6 Hz, 2H). ¹³C NMR (100 MHz, D₂O) δ (ppm): 172.47, 154.65, 147.01, 144.04, 142.38, 133.03, 131.54, 131.46, 127.42, 126.36, 125.22, 102.99, 88.60, 66.60 (2C), 62.58 (2C), 47.80 (2C), 41.44, 31.56 (2C). MS (ESI) *m/z*: 539 [M+H]⁺.

4.3. *In vitro* Akt1 kinase activity assay

The *in vitro* Akt1 kinase activity was evaluated via an HTRF assay (LANCE[®]) using the Akt kinase kit (Cisbio Bioassays, No.62ST3PEB) in 384-well plates. Each well was added Akt1, STK Substrate-biotin, tested compounds and ATP in kinase buffer (50 mM HEPES, 5 mM MgCl₂, 1 mM DTT, 0.02% NaN₃ and 0.01% BSA, pH = 7.0) in sequence, then incubated for 45 min at 25 °C. Finally, Sa-XL665 and STK Ab-Cryptate were added to stop the enzymatic step and incubated for 2 hours to finish the detection process. The ratio (665 nm/620 nm) was obtained using a microplate reader (Perkin Elmer, USA).

4.4. Cell lines and primary MCL cells

MCL cell lines JVM-2, Maver-1, SP-49, Z-138, Mino and Jeko-1 were purchased from the American Type Culture Collection (ATCC). Human MCL cells were purified from the apheresis of MCL patients after obtaining informed consent and approval by the Institutional Review Board at The University of Texas MD Anderson Cancer Center. Cells were cultured in RPMI-1640, supplemented with 10% heat-inactivated fetal bovine serum, 2% HEPES buffer and penicillin (10,000 units/mL; Sigma), streptomycin (10 mg/mL; Sigma).

4.5. Cell proliferation assay

Cell proliferation assay was performed on a panel of MCL cell lines and primary MCL cells using the CellTiter-Glo Luminescent cell viability assay kit (Promega) following the manufacturer's protocol. In short, cells were plated in 96-well plates at a density of 1×10⁴ cells/well for cell lines and 12.5×10⁴ cells/well for primary MCL cells, then treated with DMSO and different concentrations of the synthesized compounds and incubated in a humidified atmosphere with 5% CO₂ at 37 °C for 72 hours on MCL cell lines and 24 hours on primary MCL cells. IC₅₀ values were calculated using the Graphpad prism 6 software.

4.6. Cell apoptosis assay

Apoptosis was quantified by Annexin V/Propidium Iodide (PI)-binding assay. Cells were seeded

in 6-well plates with 0.5 μM , 1 μM and 5 μM of **10h** for 48 hours, or 1 μM of **10h** for 24, 48 and 72 hours. Treated cells were washed twice with cold phosphate-buffered saline (PBS) and then resuspended in 100 μL binding buffer, to which 2 μL of Annexin V-FITC and 5 μL of PI were added. The samples were gently vortexed and incubated for 15 minutes at room temperature in the dark. After addition of 200 μL binding buffer, samples were immediately analyzed by flow cytometry using a FACScan flow cytometer (Becton Dickinson, San Jose, CA). The number of apoptotic cells was determined using the Flowjo software.

4.7. Cell cycle assay

Cell cycle arrest was measured using PI staining by flow cytometry. Cells were seeded in 6-well plates with 0.5 μM , 1 μM and 5 μM of **10h** for 24 hours, then cells were harvested, washed twice with cold PBS, and subsequent fixing in cold 70% ethanol overnight at 4 $^{\circ}\text{C}$. Then samples were washed twice with PBS, followed by further treatment with 50 μL of 100 $\mu\text{g}/\text{mL}$ ribonuclease and 200 μL 50 $\mu\text{g}/\text{mL}$ PI, and finally analyzed by flow cytometry.

4.8. Western blotting

Jeko-1 cells were cultured with 0.5 μM , 1 μM and 5 μM of **10h** for 24 hours. Then cells were harvested and lysed in a lysis buffer (Cell Signaling, Danvers, MA). The cell lysates were kept on ice for 30 minutes and centrifuged at 12,000 \times rpm for 20 minutes at 4 $^{\circ}\text{C}$. The protein concentration was determined by the Bradford assay (Bio-Rad, Hercules, CA). Twenty micrograms of sample proteins were mixed with the loading buffer and separated by 10% SDS-PAGE. The proteins were then transferred onto methanol equilibrated PVDF membrane (BIO-RAD Laboratories, 162-0177), which was blocked for 1 hour in 5% nonfat dry milk in TBST (BD Bioscience, San Jose, CA). The membranes were incubated with a primary antibody overnight at 4 $^{\circ}\text{C}$. Secondary antibodies were added for 1 hour at room temperature. Finally, the membrane was visualized by ECL (Perkin Elmer Life Sciences, NE104001EA). Antibodies against PARP, cleaved caspase 3, p-AKT-308, p-AKT-473, pan-AKT, p-GSK3 β , total-GSK3 β and GAPDH were obtained from Cell Signaling.

4.9. Molecular docking

Molecular docking was performed using the Sybyl 2.0 software package and the Akt1 crystal structure (PDB: 4EKL) was retrieved from the Protein Data Bank. Protein preparation was performed by extracting the ligand, removing water molecules, adding hydrogen atoms and assigning AMBER7 FF99 charges to the protein. Compound **10h** was docked into Akt1 and the hydrogen bonds and hydrophobic interactions were observed in the model, the best conformation with the highest CScore

was selected for interaction analysis.

Acknowledgement

This work was supported by the National Natural Science Foundation of China (No. 21272140) and Projects of Shandong Science and Technology (No. 2014GSF119003).

Conflict of interest

The authors declare no conflict of interest.

References

- [1] J.R. Testa, P.N. Tsichlis, AKT signaling in normal and malignant cells, *Oncogene*, 24 (2005) 7391-7393.
- [2] C. Porta, C. Paglino, A. Mosca, Targeting PI3K/Akt/mTOR Signaling in Cancer, *Frontiers in oncology*, 4 (2014) 64.
- [3] M. Martini, M.C. De Santis, L. Braccini, F. Gulluni, E. Hirsch, PI3K/AKT signaling pathway and cancer: an updated review, *Annals of medicine*, 46 (2014) 372-383.
- [4] P. Wang, L. Zhang, Q. Hao, G. Zhao, Developments in selective small molecule ATP-targeting the serine/threonine kinase Akt/PKB, *Mini reviews in medicinal chemistry*, 11 (2011) 1093-1107.
- [5] D. Yang, P. Wang, J. Liu, H. Xing, Y. Liu, W. Xie, G. Zhao, Design, synthesis and evaluation of novel indole derivatives as AKT inhibitors, *Bioorganic & medicinal chemistry*, 22 (2014) 366-373.
- [6] J. Bhutani, A. Sheikh, A.K. Niazi, Akt inhibitors: mechanism of action and implications for anticancer therapeutics, *Infectious agents and cancer*, 8 (2013) 49.
- [7] Y. Gao, C.Y. Yuan, W. Yuan, Will targeting PI3K/Akt/mTOR signaling work in hematopoietic malignancies?, *Stem cell investigation*, 3 (2016) 31.
- [8] P.M. LoRusso, Inhibition of the PI3K/AKT/mTOR Pathway in Solid Tumors, *Journal of clinical oncology : official journal of the American Society of Clinical Oncology*, (2016).
- [9] J.A. Crowell, V.E. Steele, J.R. Fay, Targeting the AKT protein kinase for cancer chemoprevention, *Molecular cancer therapeutics*, 6 (2007) 2139-2148.
- [10] C.Y. Cheah, J.F. Seymour, M.L. Wang, Mantle Cell Lymphoma, *Journal of clinical oncology : official journal of the American Society of Clinical Oncology*, 34 (2016) 1256-1269.
- [11] Y. Chen, M. Wang, J. Romaguera, Current regimens and novel agents for mantle cell lymphoma, *Br J Haematol*, 167 (2014) 3-18.
- [12] N. Vogt, B. Dai, T. Erdmann, W.E. Berdel, G. Lenz, The molecular pathogenesis of mantle cell lymphoma, *Leukemia & Lymphoma*, (2016) 1.
- [13] P. Jares, D. Colomer, E. Campo, Genetic and molecular pathogenesis of mantle cell lymphoma: perspectives for new targeted therapeutics, *Nature Reviews Cancer*, 7 (2007) 750-762.
- [14] M. Rudelius, S. Pittaluga, S. Nishizuka, T.H. Pham, F. Fend, E.S. Jaffe, L. Quintanilla-Martinez, M. Raffeld, Constitutive activation of Akt contributes to the pathogenesis and survival of mantle cell lymphoma, *Blood*, 108 (2006) 1668-1676.
- [15] G.M. Nituлесcu, D. Margina, P. Juzenas, Q. Peng, O.T. Oлару, E. Saloustrous, C. Fenga, D. Spandidos, M. Libra, A.M. Tsatsakis, Akt inhibitors in cancer treatment: The long journey from drug discovery to clinical use (Review), *International journal of oncology*, 48 (2016) 869-885.
- [16] K.D. Freeman-Cook, C. Autry, G. Borzillo, D. Gordon, E. Barbacci-Tobin, V. Bernardo, D. Briere, T. Clark, M. Corbett, J. Jakubczak, S. Kakar, E. Knauth, B. Lippa, M.J. Luzzio, M. Mansour, G.

- Martinelli, M. Marx, K. Nelson, J. Pandit, F. Rajamohan, S. Robinson, C. Subramanyam, L. Wei, M. Wythes, J. Morris, Design of selective, ATP-competitive inhibitors of Akt, *Journal of medicinal chemistry*, 53 (2010) 4615-4622.
- [17] J.R. Bencsik, D. Xiao, J.F. Blake, N.C. Kallan, I.S. Mitchell, K.L. Spencer, R. Xu, S.L. Gloor, M. Martinson, T. Risom, R.D. Woessner, F. Dizon, W.I. Wu, G.P. Vigers, B.J. Brandhuber, N.J. Skelton, W.W. Prior, L.J. Murray, Discovery of dihydrothieno- and dihydrofuroypyrimidines as potent pan Akt inhibitors, *Bioorganic & medicinal chemistry letters*, 20 (2010) 7037-7041.
- [18] Y. Liu, Y. Yin, J. Zhang, K. Nomie, L. Zhang, D. Yang, M.L. Wang, G. Zhao, Discovery of 4-(Piperazin-1-yl)-7H-pyrrolo[2,3-d]pyrimidine Derivatives as Akt Inhibitors, *Archiv der Pharmazie*, 349 (2016) 356-362.
- [19] D.S. Levy, J.A. Kahana, R. Kumar, AKT inhibitor, GSK690693, induces growth inhibition and apoptosis in acute lymphoblastic leukemia cell lines, *Blood*, 113 (2009) 1723-1729.
- [20] F. Chang, J.T. Lee, P.M. Navolanic, L.S. Steelman, J.G. Shelton, W.L. Blalock, R.A. Franklin, J.A. McCubrey, Involvement of PI3K/Akt pathway in cell cycle progression, apoptosis, and neoplastic transformation: a target for cancer chemotherapy, *Leukemia*, 17 (2003) 590-603.
- [21] C. Stolz, G. Hess, P.S. Hahnel, F. Grabellus, S. Hoffarth, K.W. Schmid, M. Schuler, Targeting Bcl-2 family proteins modulates the sensitivity of B-cell lymphoma to rituximab-induced apoptosis, *Blood*, 112 (2008) 3312-3321.
- [22] D.S. Levy, J.A. Kahana, R. Kumar, AKT inhibitor, GSK690693, induces growth inhibition and apoptosis in acute lymphoblastic leukemia cell lines, *Blood*, 113 (2009) 1723-1729.
- [23] E.K. Han, J. Levenson, T. McGonigal, O. Shah, K. Woods, T. Hunter, V. Giranda, Y. Luo, Akt inhibitor A-443654 induces rapid Akt Ser-473 phosphorylation independent of mTORC1 inhibition, *Oncogene*, 26 (2007) 5655-5661.
- [24] N. Rhodes, D.A. Heerding, D.R. Duckett, D.J. Eberwein, V.B. Knick, T.J. Lansing, R.T. McConnell, T.M. Gilmer, S.-Y. Zhang, K. Robell, Characterization of an Akt kinase inhibitor with potent pharmacodynamic and antitumor activity, *Cancer research*, 68 (2008) 2366-2374.

Figure captions

Fig. 1. Design of the targeted compounds. A) Binding site of the ATP-competitive inhibitors; B) common features of ATP-competitive inhibitors; C) Design of the targeted compounds from the initial hit **1**

Fig. 2. Cell apoptosis and cell cycle assay for **10h** in Jeko-1 cells. A/C) Apoptosis assay of **10h** at indicated concentrations in Jeko-1 cells for 48 hours; B/D) Apoptosis assay of **10h** at 1 μ M in Jeko-1 cells for the indicated treatment periods; E) Dose-dependent activation of cleaved caspase-3 and PARP after 24 hours treatment with **10h**; F) Cell cycle analysis of **10h** at indicated concentrations in Jeko-1 cells for 24 hours.

Fig. 3. Western blot analysis, cell viability assay in patient cells and molecular modeling. A) Effects of **10h** on Akt signaling in Jeko-1 cells after 24 hours treatment; B) Relative protein expression was determined using Image J. Values were normalized to loading control; C) Cell viability assay of **10h** in primary MCL cells. Values were normalized to control; Unpaired student's t-test between **10h** and **GSK690693**-treated cells is statistically significant (* $P < 0.01$); D) Proposed binding mode of **10h** at the ATP binding site of Akt1 (PDB: 4EKL).

Highlights

- Pyrrolopyrimidine based phenylpiperidine carboxamides as potent Akt inhibitors
- Antiproliferative effects in mantle cell lymphoma cell lines and patient cells
- Induced cell apoptosis and cell cycle arrest in G₂/M phase
- Downregulated the phosphorylation of Akt downstream effector GSK3 β and S6